Hindawi Publishing Corporation
Advances in Acoustics and Vibration
Volume 2008, Article ID 495317, 9 pages
doi:10.1155/2008/495317

Research Article

Still in Womb: Intrauterine Acoustic Embedded Active Noise Control for Infant Incubators

Lichuan Liu, Shruthi Gujjula, Priya Thanigai, and Sen M. Kuo

Department of Electrical Engineering, Northern Illinois University, DeKalb, IL 60115, USA

Correspondence should be addressed to Lichuan Liu, ll24@njit.edu

Received 1 December 2007; Revised 4 February 2008; Accepted 5 March 2008

Recommended by Marek Pawelczyk

Excessive noise in neonatal care units and inside incubators can have a number of detrimental effects on an infant's health. We proposed a novel, audio-integrated approach to achieve active noise control (ANC) for infant incubators. We also presented the implementation of the robust, nonlinear filtered-X least mean M-estimate algorithm, for reducing impulsive interference in incubators. The healthcare application is further enhanced by integrating the "womb effect", that is, by using intrauterine and maternal heart sounds, proven to be beneficial to infant health, for soothing the infant and masking the residual noise. A computer model for audio-integrated noise cancellation utilizing experimentally measured transfer functions is developed for simulations using real medical equipment noise. The simulation of the audio integrated ANC system produced optimal results and the system was further validated by real-time experiments to be robust and efficient.

1. INTRODUCTION

Neonatal intensive care units (NICU) house and treat premature infants until their organ systems are considered fully developed. These infants are enclosed in incubators, as shown in Figure 1, that monitor their vital statistics and ensure that environmental conditions are maintained at optimum levels. The incubators create the precise and consistent environment [1], such as temperature and humidity, controlled by microprocessor. However, according to the American Academy of Pediatrics [2], high noise levels are common in the NICU and in incubators, causing considerable auditory damage to preterm infants [3]. The noise is typically due to ventilation or breathing equipment and human activity. Figure 2 is an example of the real incubator noise in time domain with segments marked by impulse due to respiratory pumps and the background equipment hum. The consequences of exposing infants to incubator noise vary from short-term effects such as sleep disturbance to long-term effects such as delayed speech development. To reduce medical equipment noise and external noise from the NICU, passive control systems such as absorbers [4] are not always efficient. This puts forth a need for an active noise control (ANC) system that can cancel noise inside the incubator adaptively [5, 6]. Another approach to create a healthier ambience in NICUs is the introduction of intrauterine audio into the incubator that allows the infant to feel comforted. Intrauterine audio is a combination of low-frequency sounds from the womb and includes the sound of the muffled heartbeat which can be heard distinctly in the background.

However, neither playing soothing audio nor applying an ANC system is individually efficient creating the need for an integrated system that can reduce harmful equipment noise while simultaneously playing beneficial intrauterine audio. To achieve this end, this paper proposes an innovative application for neonatal healthcare—the intrauterine acoustics embedded active noise controller. The integrated system aims at recreating prenatal ambience for premature infants who are required to spend extended periods enclosed inside infant incubators.

Section 2 of the paper discusses the positive effects of playing uterine audio to premature infants. These positive effects are both medical and psychological, and reflect results from studies carried out over the last three decades. Section 3 focuses on developing an ANC system utilizing the filtered-X least mean square (FXLMS) algorithm for cancellation of broadband noise using transfer functions

Figure 1: Mobile incubator unit: Giraffe Incubator by GE Healthcare.

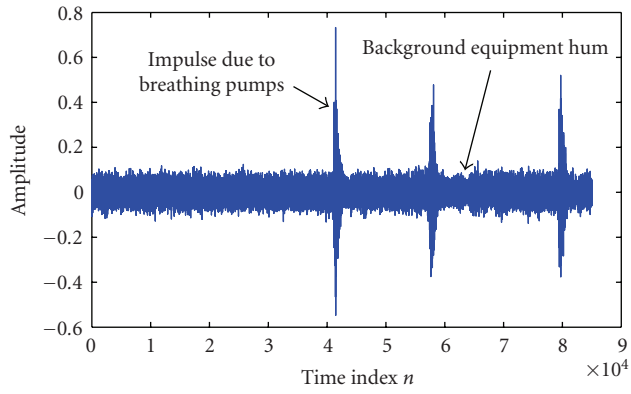

Figure 2: Example wave form of incubator noise, sampling frequency $f_s = 4$ KHz.

measured from the real GE Healthcare Girraffe incubator. The laboratory setup was modeled using the same incubator shown in Figure 1. Section 4 introduces the novel filtered-X least mean M-estimate (FXLMM) algorithm that is found to be statistically robust in the presence of impulsive interference in the input. Section 5 outlines the audio-integration algorithm that introduces intrauterine audio and allows it to be played simultaneously while the ANC system is in operation. This integration serves two important purposes—it provides a potential health benefit for infants by utilizing womb sounds as heard by the infant and also masks the residual noise after noise cancellation has been performed. The algorithm is intended to prevent interference from the soothing audio on the performance of the ANC algorithm and ensures that the audio is not cancelled by the ANC system. The audio interference cancellation filter also performs online modeling of the secondary path to enhance the performance of the ANC system. Section 6 shows the simulation and real time experiment results.

2. A STUDY OF NEONATAL RESPONSE TO UTERINE SOUNDS

This section briefly reviews that the numerous benefits intrauterine audio has on neonatal growth from [5]. It is widely accepted that the brain of the fetus develops while it is inside the womb. An infant's ears begin to develop when it is around eight weeks old and can be considered fully developed by the twenty-fourth week. The development of the inner ears and the nerve endings from the brain is so advanced that the baby can hear the muffled sounds of the heartbeat and the blood flowing through the umbilical cord. The human cochlear system, which is considered fully developed by the twenty-fourth week, transforms acoustic vibrations into nervous influx allowing infants to have an understanding of rhythm at a very early stage [7]. These sounds form an imprint on the fetal brain and it has been verified that post birth, the infant is comforted while listening to it.

Playing soothing audio has always been known to relieve stress and has in recent years become an established form of therapy. There have been a number of studies that indicate that music has a positive impact on premature infants yet the kind of audio to be played is contentious. The various available options include playing nature sounds, live and recorded music. But "womb music" has consistently been considered the most favorable choice. According to [7] the womb is not a silent place and is typically awash with sounds. Sounds that are heard inside the uterus include maternal heartbeat, respiration, intestinal gurgling and sounds from blood vessels. The maternal heartbeat heard by the infant is a muffled version of the original as it passes through layers of tissues before reaching the infant. A study conducted by Rosner and Doherty in [8] states that "playing prerecorded intrauterine sounds to newborns reportedly soothes the babies." The study concluded that 90% of infants who listened to intrauterine audio were calmed down significantly.

In another study conducted by Murooka et al. [9], the authors used a piezoelectric microphone to record and analyze intrauterine sounds. The sounds were found to be mainly from blood vessels and were found to produce a calming effect on 86% of the infants, and 30% of the infants were found to have increased sleep cycles. The authors asserted that playing such sounds externally recreates the "in-utero" ambience for infants [9]. A pioneering study conducted by Salk [10] exposed neonates to prerecorded maternal heartbeat and concluded that test infants showed increased weight gain and food intake. Flowers, McCain, and Hilker combined uterine sounds with soft ballads and tested the impact of music on nine African-American premature infants. The infants displayed improvement in respiration rate, oxygen saturation, and time spent in sleeping [11].

This paper therefore proposes the utilization of sound files from a commercially available product—the Baby Sleep System [12]. The soothing audio consists of intrauterine heartbeat recorded through a condenser microphone, which is a very accurate representation of uterine sounds as heard by the infant. The heartbeats were taken at 72 beats per minute, the rate of a relaxed adult heart. They were combined

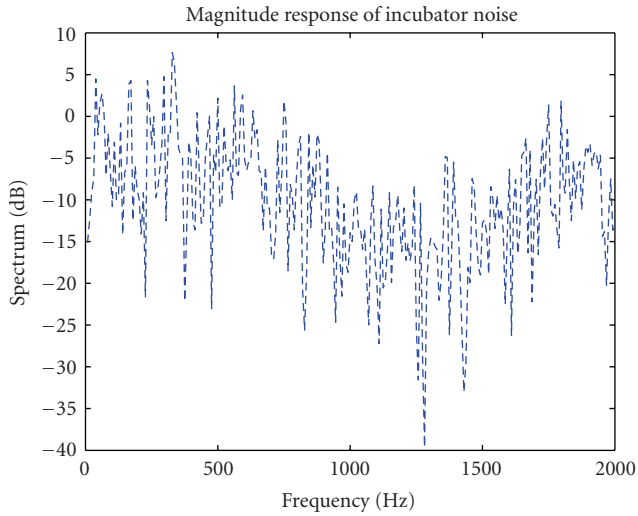

Figure 3: Magnitude response of the incubator wideband noise.

with the sound of blood and fluid movement to produce an "in-utero" effect for the infant. This audio was incorporated along with the ANC system and serves two main purposes. The ANC system is optimized to cancel equipment and external NICU noise to the maximum possible extent. The audio integration allows for the soothing audio to be played continuously without interfering with the ANC system. Also, the integrated system can be considered cost effective as the power amplifiers and loudspeakers used by the ANC system can be used for playing the soothing audio, thus maximizing the utility of resources.

3. ACTIVE NOISE CONTROL FOR THE INCUBATORS

The noise in incubator can be classified as broadband noise because it covers a wide range of frequencies [13]. The noise sources are some medical equipments in the ICU, such as a blowers, nebulizers, humidifiers, and pumps. Figure 3 shows the magnitude spectrum of the recorded sample of broadband incubator noise. We can find that the power of the noise is spread over a wide spectrum of the noise signal. The ANC systems can be used to cancel this high-power wideband noise.

ANC is based on the principle of untilizing destructive interference to cancel unwanted noise. The objective of an ANC system is to generate an "antinoise" to cancel the primary noise. The amount of noise which can be cancelled depends on the accuracy of the amplitude and phase of this antinoise [14].

The block diagram of a feedforward broadband ANC system using the FXLMS algorithm is illustrated in Figure 4, where $P(z)$ is the transfer function of the primary path from the noise source to the error microphones, $S(z)$ is the transfer function of secondary path and $\hat{S}(z)$ is its estimate. The primary noise $d(n)$ inside the incubator is cancelled by the antinoise $y(n)$ generated by the adaptive filter $W(z)$. The antinoise is produced by the secondary loudspeakers and $e(n)$ is the residual noise picked up by the error microphone.

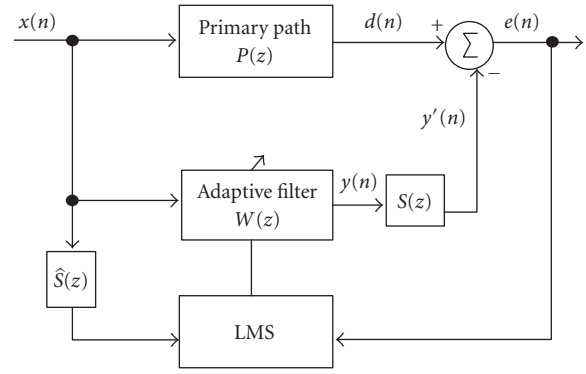

Figure 4: Block diagram of ANC system with the FXLMS algorithm.

In Figure 4, $S(z)$ which is the secondary path between $e(n)$ and $y(n)$, includes the secondary loudspeakers, error microphones, and acoustic path between the loudspeakers and the error microphones. The secondary path is modeled offline and retained during the online operation of ANC. The estimate compensates for the secondary-path effects [15].

The output of the adaptive filter can be represented as [15]

$$y(n) = \mathbf{w}^T(n)\mathbf{x}(n), \tag{1}$$

where $\mathbf{w}(n) = [w_0(n)\ w_1(n) \cdots w_{L-1}(n)]^T$ is the coefficient vector of the adaptive filter $W(z)$ and $\mathbf{x}(n) = [x(n)\ x(n-1) \cdots x(n-L+1)]^T$ is the $L \times 1$ reference signal vector. The signal $y(n)$ is filtered through the secondary path $S(z)$ and is subtracted from the primary noise $d(n)$ to generate the residual error $e(n)$. The equations for simulation are given by

$$\begin{aligned} d(n) &= p(n) * x(n), \\ y'(n) &= s(n) * y(n), \\ e(n) = d(n) - y'(n) &= d(n) - s(n) * [\mathbf{w}^T(n)\mathbf{x}(n)], \end{aligned} \tag{2}$$

where $*$ denotes the convolution operator, and $p(n)$ and $s(n)$ are the primary and secondary path responses, respectively. All these operations are carried out by the system internally and the signals picked up in real-time ANC are the reference signal $x(n)$ and the residual error $e(n)$. For the adaptive filter, the weight update equation is

$$\mathbf{w}(n+1) = \mathbf{w}(n) + \mu e(n)\mathbf{x}'(n), \tag{3}$$

μ is the step size; $\mathbf{x}'(n) = [x'(n)\ x'(n-1) \cdots x'(n-L+1)]^T$ is the reference signal vector $\mathbf{x}(n)$ filtered by the secondary path model $\hat{S}(z)$,

$$x'(n) = \hat{s}(n) * x(n), \tag{4}$$

where $\hat{s}(n)$ is an accurate estimate of $s(n)$.

The experimental setup is shown in Figure 5. One microphone is placed on either side of the infant head. The outputs from both are analyzed by a spectrum analyzer.

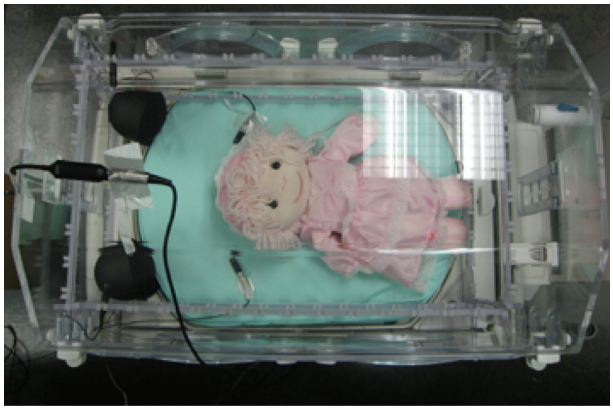

Figure 5: Experiment setup by using the GE Healthcare Giraffe Incubator.

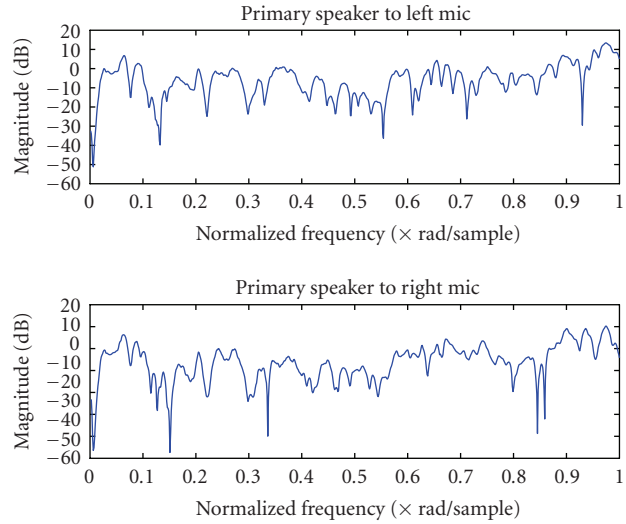

Figure 6: Magnitude responses of the primary paths.

The cancelling loudspeakers are placed in the incubator, and can be seen behind the infant head. Typically the offline modeling of the secondary paths from the cancelling loudspeakers to the error microphones is using adaptive filters with the least mean square algorithm. The magnitude responses of the primary paths $P(z)$ from the experimental setup are shown in Figure 6.

Typically, white noise is used for adaptive system identification. But it is found to be annoying especially in sensitive environments like the NICU. The proposed method utilizes offline modeling approach. Nature's sound, in this case, the sound of a flowing stream is used. Nature's sounds are preferred owing to their flat spectrum and their pleasing effect on the listener. The secondary paths estimator converged for a filter length of 30. Satisfactory results of offline modeling are shown in Figure 7.

4. NONLINEAR ALGORITHM FOR IMPULSE NOISE SUPPRESSION

The performance of the linear adaptive filters degrade dramatically in the presence of impulse noise, therefore nonlinear algorithms are capable of reducing the adverse effects [16]. The FXLMM algorithm is a simple and robust method. It employs the mean M-estimation error objective function and is capable of performing effectively in impulsive environment [17–19].

The objective of the adaptive filter $W(z)$ is to minimize the least M-estimate function criterion $\rho[e(i)]$ where $\rho(\cdot)$ is the M-estimate function. The coefficient vector $\mathbf{w}(n)$ is updated in the negative direction of the gradient vector

$$\mathbf{w}(n+1) = \mathbf{w}(n) - \mu \nabla J_{MP} \tag{5}$$

and the objective function is

$$J_{MP} \equiv E[\rho[e(n)]] \cong \rho[e(n)], \tag{6}$$

where $E[\cdot]$ is the expectation operator, $\rho(\cdot)$ is chosen to be the Hampel three-part redescending M-estimate function, which is well known for its computational simplicity. It defines as

$$\rho[e(n)] = \begin{cases} \dfrac{e^2(n)}{2}, & 0 \le |e(n)| < \xi, \\ \xi|e(n)| - \dfrac{\xi^2}{2}, & \xi \le |e(n)| < \Delta_1, \\ \dfrac{\xi}{2(\Delta_1+\Delta_2)} - \dfrac{\xi^2}{2} + \dfrac{(\xi|e(n)| - \Delta_2)^2}{2(\Delta_1-\Delta_2)}, & \Delta_1 \le |e(n)| < \Delta_2, \\ \dfrac{\xi}{2(\Delta_1+\Delta_2)} - \dfrac{\xi^2}{2}, & \Delta_2 \le |e(n)|, \end{cases} \tag{7}$$

where ξ, Δ_1, and Δ_2 are the threshold parameters.

The objective function is minimized by

$$\nabla J_{MP} = \frac{\partial J_{MP(n)}}{\partial \mathbf{w}(n)} = \frac{\partial \rho[e(n)]}{\partial e(n)} \frac{\partial e(n)}{\partial \mathbf{w}(n)}. \tag{8}$$

Let $\psi[e(n)]$ be the first-order partial derivative of $\rho[e(n)]$, (8) becomes

$$\begin{aligned} \nabla J_{MP} &= \psi[e(n)] \frac{\partial e(n)}{\partial \mathbf{w}(n)} = \psi[e(n)][-s(n) * \mathbf{x}(n)] \\ &= -q[e(n)]e(n)[s(n) * \mathbf{x}(n)]. \end{aligned} \tag{9}$$

Define $q[e(n)] \equiv \psi[e(n)]/e(n)$ as the weight function. Since $s(n)$ is the impulse response of the secondary path and not available directly, we use its estimation to calculate the gradient,

$$\nabla J_{MP} \cong -q[e(n)]e(n)[\hat{s}(n) * \mathbf{x}(n)] = -q[e(n)]e(n)\mathbf{x}'(n). \tag{10}$$

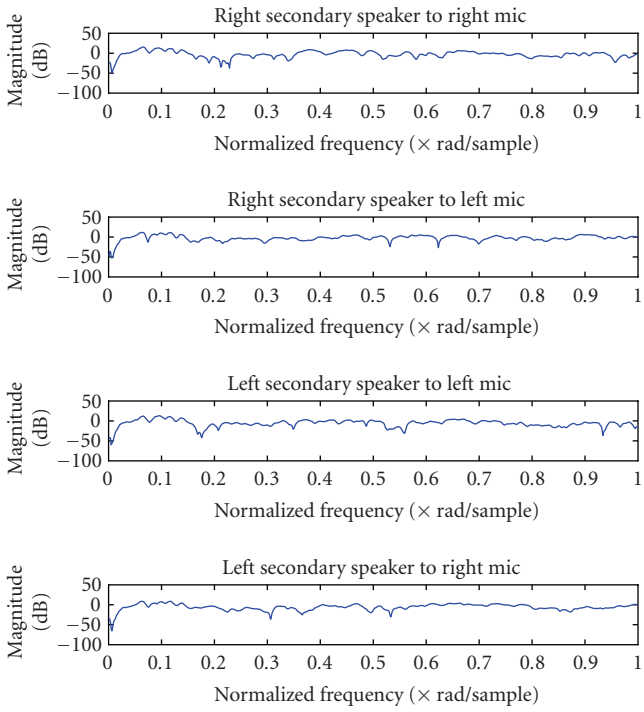

Figure 7: Magnitude responses of the secondary paths.

Substituting (10) into (5), we can get the weight vector update equation as

$$\mathbf{w}(n+1) = \mathbf{w}(n) + \mu q[e(n)]e(n)\mathbf{x}'(n), \tag{11}$$

where μ is the step size parameter. Equation (11) is known as the least M-estimate algorithm and can be viewed as a generalization of the LMS algorithm. It becomes identical to the LMS algorithm when noise $e(n)$ is less than a threshold ξ. When the signal error $e(n) > \xi$, $q[e(n)]$ in (11) decreases and reaches 0 when $e(n) > \Delta_2$. Thus, the least M-estimate algorithm is capable of reducing the effect of large signal error during the updating process [17].

5. INTRAUTERINE ACOUSTICS EMBEDDED ACTIVE NOISE CONTROLLER

This section develops an algorithm that can integrate the "comfort" audio with the existing ANC system, and provide an environment that is capable of improving the health of the infant by masking the undesired residual noise. The comfort audio used is a combination of maternal heartbeat and other intrauterine sounds [12]. Research has proven that playing womb sound to infant in incubator showed significant benefit in the respiration rate, sleep cycle, and oxygen saturation [11]. Unfortunately, there are two main issues with the integration of audio to the ANC system need to be considered: first, the audio signal can act as interference to the ANC system and impede proper adaptation; and second, the ANC system can cancel the intended soothing sound. Hence, a method must be devised to subtract the audio from error signal before it is used to update the

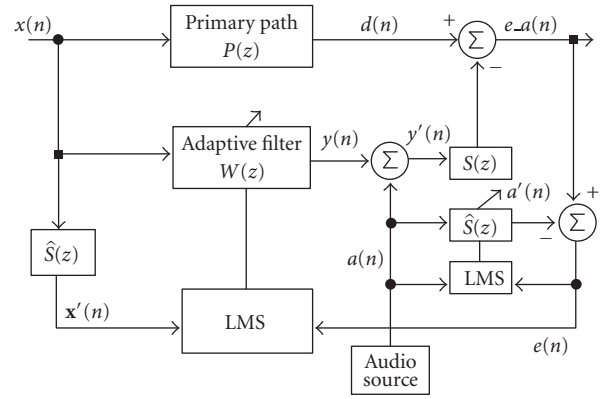

Figure 8: Block diagram of the audio-integrated ANC system.

coefficients of the adaptive filter [20]. The block diagram of the audio integration algorithm is shown in Figure 8. The soothing audio $a(n)$ is added to $y(n)$ and can be heard by the infant inside the incubator.

At the acoustic summing junction, the antinoise $y'(n)$ and the primary noise $d(n)$ are combined to produce the residual error $e\_a(n)$. It contains the true error (residual noise) $e(n)$ and the component of audio. Therefore, by subtracting the audio from the residual error $e\_a(n)$, we can get the true error, then the true error is used to update the weight vector of the adaptive filter $W(z)$. It should be noted that the audio signal passed the secondary path, and filtered by $S(z)$, then it is subtracted. The z transform of residual error $e\_a(n)$ can be expressed as [21]

$$E\_A(z) = D(z) - S(z)[Y(z) + A(z)]. \tag{12}$$

The adaptive filter $\hat{S}(z)$ is used to cancel the audio interference on the performance of $W(z)$. This filter generates

$$E(z) = E\_A(z) + \hat{S}(z)A(z). \tag{13}$$

Then we can get the following equation by substituting (12) into (13):

$$E(z) = D(z) - S(z)Y(z). \tag{14}$$

We assume that $S(z) = \hat{S}(z)$ and the audio is uncorrelated with the primary noise. Then (13) can be expressed in time domain as

$$e(n) = d(n) - [y(n) * s(n)] \tag{15}$$

which is the true error used to update $W(z)$ by using the FXLMS system.

The main advantage of this algorithm lies in its ability to model the secondary path online. This involves the estimation of the secondary path in parallel with the operation of the ANC system. The $S(z)$ filter is modeled through a system identification scheme. It uses soothing audio as the reference signal and treats the secondary path as the unknown system. This makes the algorithm sensitive to time-varying secondary paths.

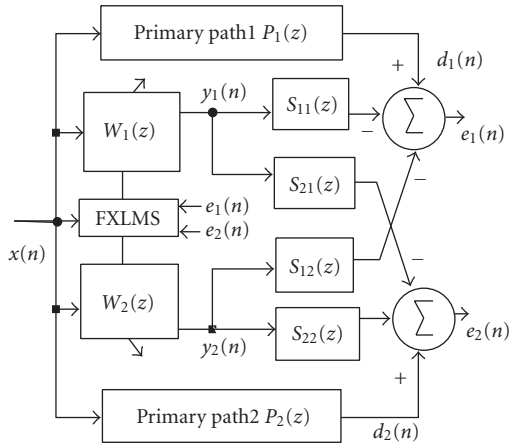

Figure 9: Block Diagram of the $1 \times 2 \times 2$ FXLMS algorithm.

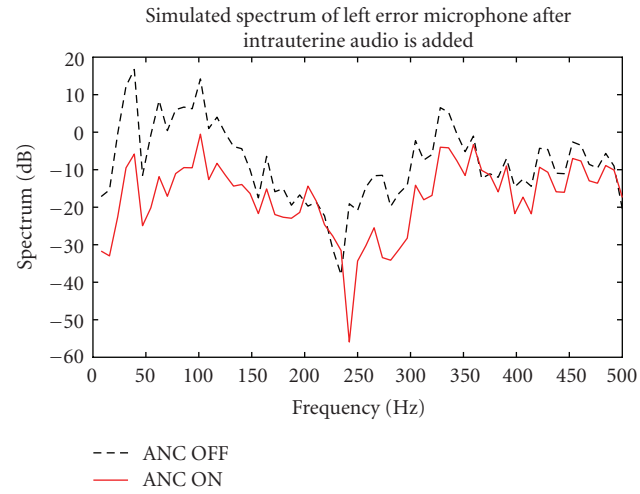

Figure 10: Simulated spectra at left error microphone before (ANC OFF) and after (ANC ON) active noise control.

The key advantages of the intrauterine acoustic embedded ANC system can be summarized as follows. (i) It re-establishes pre-natal ambience thus fostering infant health. (ii) The secondary path is modeled online making the system more receptive to changes in the environment. (iii) It is successful in masking residual error and in preventing the audio from interfering with the updation. (iv) The audio integration does not require supplementary hardware, existing speakers and power amplifier of the ANC system can be used making it cost effective.

6. SIMULATION AND EXPERIMENT RESULTS

6.1. Multichannel FXLMS algorithm

In the previous sections, we described the single channel ANC system. In this section, an example of multichannel ANC system, $1 \times 2 \times 2$ FXLMS algorithm is used for real experiment. Figure 9 shows the multichannel feedforward ANC system using the $1 \times 2 \times 2$ FXLMS algorithm. In this system, two secondary speakers and two error microphones are used independently. These two error microphones pick up the residual errors $e_1(n)$ and $e_2(n)$ at different positions, thus able to form two individual quiet zones centered at the error microphones. The ANC algorithm used two adaptive filters $W_1(z)$ and $W_2(z)$ to generate antinoise $y_1(n)$ and $y_2(n)$ to drive the two independent secondary speakers. In Figure 9, $d_1(n)$ and $d_2(n)$ are the primary noises to be cancelled, $S_{11}(z)$, $S_{12}(z)$, $S_{21}(z)$, and $S_{22}(z)$ are the secondary path transfer functions, and $P_1(z)$ and $P_2(z)$ are the primary path transfer functions.

The multichannel FXLMS algorithm is summarized as follows:

$$y_i(n) = \mathbf{w}_i^T(n)\mathbf{x}(n), \quad i = 1, 2,$$

$$\mathbf{w}_i(n+1) = \mathbf{w}_i(n) + \mu_i\left[e_i(n)\mathbf{x}(n) * \hat{s}_{i1}(n) + e_i(n)\mathbf{x}(n) * \hat{s}_{i2}(n)\right], \quad i = 1, 2, \tag{16}$$

where $\mathbf{w}_1(n)$ and $\mathbf{w}_2(n)$ are weight vectors of the adaptive filters $W_1(z)$ and $W_2(z)$, respectively, μ_1 and μ_2 are the step sizes, $\hat{s}_{11}(n)$, $\hat{s}_{12}(n)$, $\hat{s}_{21}(n)$, and $\hat{s}_{22}(n)$ are the impulse responses of $\hat{S}_{11}(z)$, $\hat{S}_{12}(z)$, $\hat{S}_{21}(z)$, and $\hat{S}_{22}(z)$, respectively.

Similar to the multichannel ANC system (as shown in Figure 9), we extended the single-channel audio-integrated ANC system (as shown in Figure 8) into a $1 \times 2 \times 2$ multichanel system. In this multichannel intrauterine acoustics embedded ANC system, the two adaptive filters $W_1(z)$ and $W_2(z)$ are used to update the two antinoise $y_1(n)$ and $y_2(n)$.

6.2. Simulation results

To evaluate the performance of the innovative intrauterine acoustic embedded ANC, we investigate the noise cancellation achievement through simulation and real time experiment.

In the simulation, we apply the intrauterine acoustics embedded ANC system described in Section 6.1. The input reference noise is taken from an incubator noise audio file at first. The ANC system is simulated with measured $P_1(z)$, $P_2(z)$, $S_{11}(z)$, $S_{12}(z)$, $S_{21}(z)$, and $S_{22}(z)$. A 60-tap filter with step size of 0.1 is used for the adaptive noise cancellation filter $W_1(z)$ and $W_2(z)$. The residual noise is found to be 16 dB lower than the input on average. The plots illustrating the spectra of noise before (ANC OFF) and after (ANC ON) cancellation at left error microphone and right error microphone after assigning intrauterine audio are shown in Figures 10 and 11.

To demonstrate the impulse noise suppress by nonlinear algorithms, the noise signal is interspersed with high-amplitude random impulses (30 dB higher than background). The impulses are at time $n = 40000$, 52000, and 64000 and last for a length of 100 samples. The FXLMM algorithm was implemented for the audio-integrated ANC

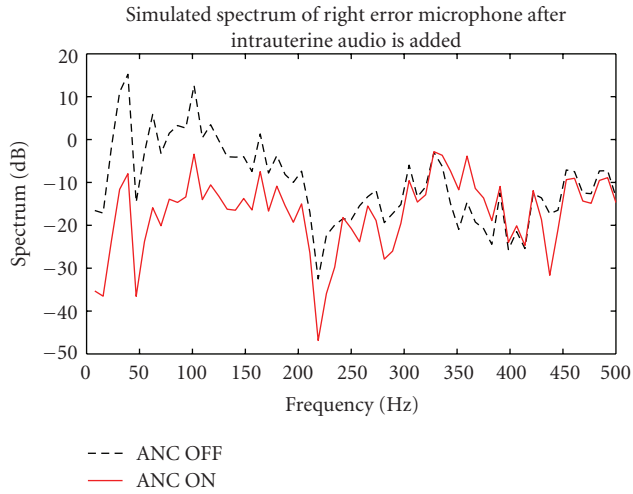

Figure 11: Simulated spectra at right error microphone before (ANC OFF) and after (ANC ON) active noise control.

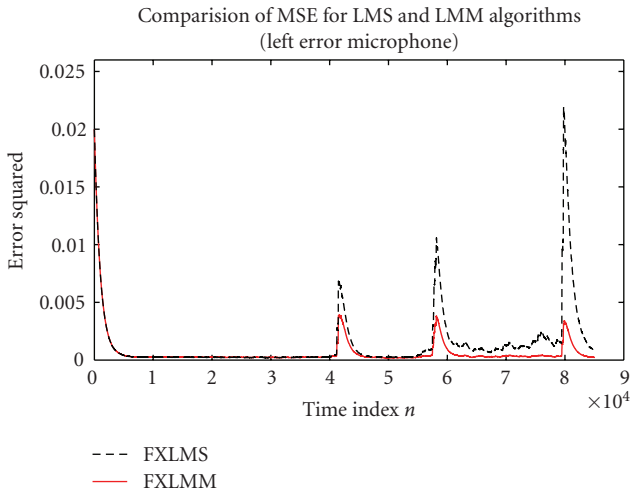

Figure 12: Learning curves at left error microphone for the FXLMS and FXLMM algorithms ($\mu = 0.0007$, impulse occurred at $n = 40000$, 62000, and 64000).

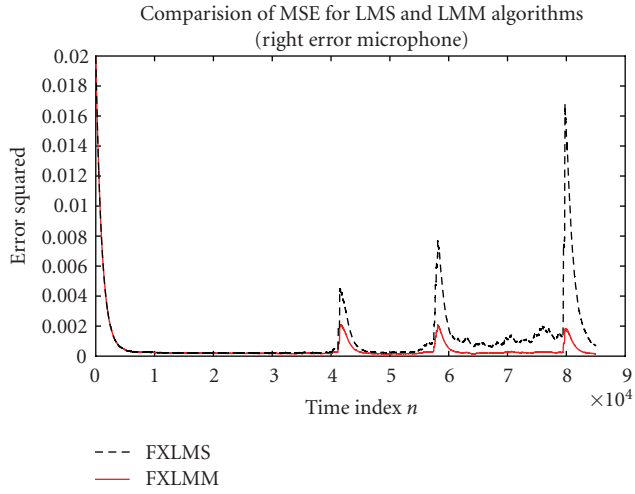

Figure 13: Learning curves at right error microphone for the FXLMS and FXLMM algorithms ($\mu = 0.0007$, impulse occurred at $n = 40000$, 62000, and 64000).

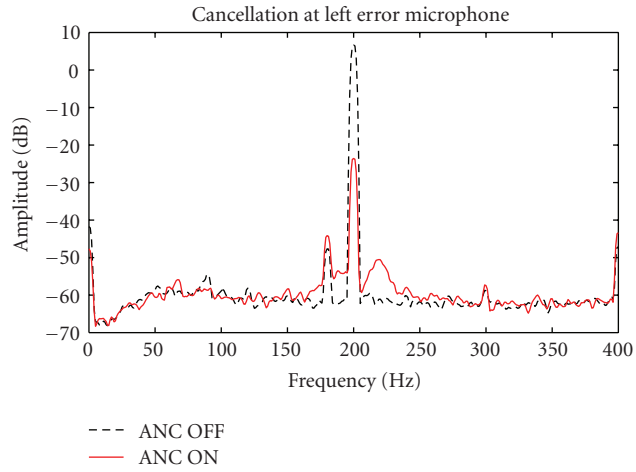

Figure 14: Real-time noise cancellation at left error microphone in the incubator.

system. The probabilities θ_ξ, θ_{Δ_1}, and θ_{Δ_2} for determining the threshold were taken to be 0.05, 0.025, and 0.005, respectively, for 95%, 97.5%, and 99.5% confidence that the error vector was in the interval $[0, \xi]$, $[0, \Delta_1]$, and $[0, \Delta_2]$, respectively [17]. A 60-tap adaptive filter with a step size of 0.0007 was implemented. The results of incubator noise cancellation are shown in Figures 12 and 13.

The simulation results show that the FXLMM algorithm behaves in an identical manner to the FXLMS algorithm until before the impulses are encountered. The FXLMS algorithm, however, exhibits a degraded system performance with a very high mean-squared error (MSE) in the presence of impulses. The FXLMM algorithm is found to be more robust while handling impulses. Comparing the MSE plots of the two algorithms shows that the FXLMM algorithm has superior performance in the presence of impulses and is more effective in suppressing the adverse influence of impulse noise.

6.3. *Real-time experiment results*

A real-time experiment is set up as shown in Figure 5 with the real GE Healthcare incubator, we use a 200 Hz sinusoidal signal generated by a loudspeaker as the primary noise (60 dB higher than the background), two antinoise loudspeakers are fixed in the incubator, two error microphones are placed near baby's ears to pick up the noise residue, the primary microphone is set on the top of the incubator in order to collect the primary noise signal. A TI TMS320C30 DSP is used for the ANC system. The assembly language is used for software developing in order to achieve the real-time processing requirement [22]. For the real-time experiment setup, the sampling frequency is 1.938 KHz, two 220-tap filters with the convergence factor of 0.0003 were used for the adaptive noise cancellation filters $W_1(z)$ and $W_2(z)$.

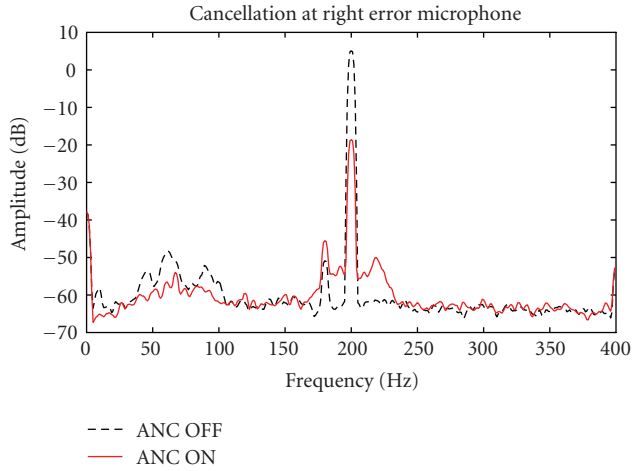

Figure 15: Real time noise cancellation at right error microphone in the incubator.

The real-time noise cancellation results based on the real time experiment are shown in Figures 14 and 15. By comparing the spectra of the noise before and after cancellation, we can find that the residual noises are 30.231 dB lower than the original noise at the left error microphone and 23.685 dB lower at the right error microphone. After the ANC system, the high power noise is dramatically reduced into an acceptable range and not harmful any more.

7. CONCLUSION

In this paper, a novel neonatal healthcare application, the intrauterine acoustics embedded active noise controller, has been presented. The integration algorithm created a beneficial environment for the infant and allowed the residual noise from the ANC system to be masked. The ANC system involved an adaptive method of noise cancellation using the statistically robust FXLMM algorithm. It allowed for stable operation of the ANC system in the presence of impulsive interference in the input. Real transfer functions measured from a laboratory setup were used to develop a computer model for simulation of the ANC system. The integration algorithm was proven to be highly advantageous as it allows the secondary path to be modeled online making the system more sensitive to changes in the environment. The real time controller was found to be cost effective and displayed stable performance in the real incubator.

REFERENCES

[1] G. Healthcare, Incubator the better care by design, http://www.gehealthcare.com/usen/perinatal/micro_environments/giraffe/products/giraffeincubator_fnb.html.

[2] R. A. Etzel, S. J. Balk, C. F. Bearer, M. D. Miller, and K. M. Shea, "Noise: a hazard for the fetus and newborn," *Pediatrics*, vol. 100, no. 4, pp. 724–727, 1997.

[3] P. Bremmer, J. F. Byers, and E. Kiehl, "Noise and the prematureinfant: physilological effects and practice impications," *Journal of Obstetric, Gynecologic, & Neonatal Nursing*, vol. 32, no. 4, pp. 447–454, 2003.

[4] A. N. Johnson, "Neonatal response to control of noise inside the incubator," *Pediatric Nursing*, vol. 27, no. 6, pp. 600–605, 2001.

[5] P. Thanigai, S. M. Kuo, and R. Yenduri, "Nonlinear active noise control for infant incubators in neo-natal intensive care units," in *Proceedings of the IEEE International Conference on Acoustics, Speech and Signal Processing (ICASSP '07)*, vol. 1, pp. 109–112, Honolulu, Hawaii, USA, April 2007.

[6] P. Thanigai and S. M. Kuo, "Intrauterine acoustic embedded active noise controller," in *Proceedings of the IEEE International Conference on Control Applications (CCA '07)*, pp. 1359–1364, Singapore, October 2007.

[7] G. E. Whitwell, "The importance of prenatal sound and music," http://www.birthpsychology.com/lifebefore/sound1.html.

[8] B. S. Rosner and N. E. Doherty, "The response of neonates to intra uterine sounds," *Developmental Medicine and Child Neurology*, vol. 21, pp. 723–729, 1979.

[9] H. Murooka, Y. Koie, and N. Suda, "Analysis of intrauterine sounds and their tranquilizing effects on the newborn infant," *Journal de Gynecologie, Obstetrique et Biologie de la Reproduction*, vol. 5, pp. 367–376, 1976.

[10] J. D. Tulloch, H. L. Jacobs, D. G. Prugh, and W. A. Greene, "Normal heartbeat sound and the behavior of newborn infants—a replication study," *Psychosomatic Medicine*, vol. 26, no. 6, pp. 661–670, 1964.

[11] J. M. Standley, "A meta-analysis of the efficacy of music therapy for premature infants," *Journal of Pediatric Nursing*, vol. 17, no. 2, pp. 107–113, 2002.

[12] The miracle baby sleep system, http://www.babysleepsystem.com/index.htm.

[13] W. B. Carvalho, M. L. G. Pedreira, and M. A. L. de Aguiar, "Noise level in a pediatric intensive care unit," *Jornal de Pediatria*, vol. 81, no. 6, pp. 485–498, 2005.

[14] S. M. Kuo and D. R. Morgan, "Active noise control: a tutorial review," *Proceedings of the IEEE*, vol. 87, no. 6, pp. 943–973, 1999.

[15] S. M. Kuo and D. R. Morgan, *Active Noise Control Systems Algorithms and DSP Implementations*, John Wiley & Sons, New York, NY, USA, 1996.

[16] P. J. Rousseeuw and A. M. Leroy, *Robust Regression and Outlier Detection*, John Wiley & Sons, New York, NY, USA, 1987.

[17] Y. Zou, S.-C. Chan, and T.-S. Ng, "Least mean M-estimate algorithms for robust adaptive filtering in impulse noise," *IEEE Transactions on Circuits and Systems II*, vol. 47, no. 12, pp. 1564–1569, 2000.

[18] Y. Zou, S.-C. Chan, and T.-S. Ng, "A robust M-estimate adaptive filter for impulse noise suppression," in *Proceedings of the IEEE International Conference on Acoustics, Speech, and Signal Processing (ICASSP '99)*, vol. 4, pp. 1765–1768, Phoenix, Ariz, USA, May 1999.

[19] S.-C. Chan and Y.-X. Zou, "A recursive least M-estimate algorithm for robust adaptive filtering in impulsive noise: fast algorithm and convergence performance analysis," *IEEE Transactions on Signal Processing*, vol. 52, no. 4, pp. 975–991, 2004.

[20] M. Zhang, H. Lan, and W. Ser, "A robust online secondary path modeling method with auxiliary noise power scheduling strategy and norm constraint manipulation," *IEEE Transactions on Speech and Audio Processing*, vol. 11, no. 1, pp. 45–53, 2003.

[21] W. S. Gan and S. M. Kuo, "An integrated audio and active noise control headsets," *IEEE Transactions on Consumer Electronics*, vol. 48, no. 2, pp. 242–247, 2002.

[22] S. M. Kuo, B. H. Lee, and W. Tian, *Real-Time Digital Signal Processing Implementations and Applications*, John Wiley & Sons, Hoboken, NJ, USA, 2006.